DOI: 10.1002/ejic.201100115

$Li_2Sr_4[Si_2N_5]N$ – A Layered Lithium Nitridosilicate Nitride

Saskia Lupart,[a] Sandro Pagano,[a] Oliver Oeckler,[a] and Wolfgang Schnick*[a]

Dedicated to Professor Hanskarl Müller-Buschbaum on the occasion of his 80th birthday

Keywords: Solid-state structures / Lithium / Silicon / Nitridosilicates / Density functional calculations

The quaternary alkaline earth nitridosilicate nitride $Li_2Sr_4[Si_2N_5]N$ has been synthesized at 900 °C using liquid lithium as fluxing agent in weld-shut tantalum ampoules. The structure of $Li_2Sr_4[Si_2N_5]N$ {space group $I\bar{4}m2$ [no. 119, a = 751.46(11), c = 1508.9(3) pm, Z = 4, $R1$ = 0.049, $wR2$ = 0.135, 499 data, 41 parameters]} is built up from vertex sharing $[SiN_4]$ tetrahedra forming layers which can be derived from the apophyllite structure type. According to the condensation degree of κ = 2:5 discrete N^{3-} ions which are coordinated by five Sr^{2+} and one Li^+ site occur besides the silicate layers in the crystal structure. The electronic structure and chemical bonding in $Li_2Sr_4[Si_2N_5]N$ has been analyzed by Madelung calculations (MAPLE) and DFT (VASP) calculations.

Introduction

Both from an academic as well as an industrial point of view nitridosilicates and related compounds (e.g. SiONs and SiAlONs) are interesting materials due to their outstanding chemical and physical properties (e.g. luminescence or lithium ion conductivity).[1–3] Nitridosilicates can be formally derived from oxosilicates by substituting N for O, which allows more extended structural possibilities. As the structural chemistry of oxygen in silicates is limited to terminal $O^{[1]}$ or bridging $O^{[2]}$ atom positions,[4] a higher crosslinking can be achieved by substituting O for N, which allows connecting up to four neighboring tetrahedral centers yielding even ammonium type character for N. Typical structures with $N,^{[1]}$ $N,^{[2]}$ $N^{[3]}$ or $N^{[4]}$ functionalities have been summarized in a recent review and include examples such as $M_2Si_5N_8$ with M = Sr, Ba ($N,^{[2]}$ $N^{[3]}$), $MSi_2O_2N_2$ with M = Ca, Sr, Ba ($N^{[3]}$), γ-Si_3N_4 ($N^{[4]}$) or $MYbSi_4N_7$ with M = Eu, Sr, Ba ($N,^{[2]}$ $N^{[4]}$).[3] In addition, edge-sharing tetrahedra have been observed in nitridosilicates, whereas for oxosilicates they have exclusively been postulated for fibrous SiO_2.[5] However, the existence of the latter compound has been controversially discussed.

Most of the nitridosilicates reported so far, have been synthesized employing high temperatures (1400–1600 °C) and exhibit predominantly three-dimensional silicate networks made up of $[SiN_4]$ tetrahedra. This observation is probably due to the rather harsh syntheses conditions that favor formation of more stable network structures.[6–10] Recently, a novel synthetic approach has been reported using sodium melts as fluxing agent. Thereby, the nitridosilicate $Ba_5Si_2N_6$ which consists of exclusively edge-sharing $[Si_2N_6]^{10-}$ bow-tie units could be synthesized at lower temperatures.[11] The employment of liquid sodium as fluxing agent at lower temperatures also afforded the compounds $MSiN_2$ (M = Ca, Sr, Ba).[9] Recently, we reported about a variation of this method using liquid lithium in weld-shut tantalum ampoules, which exhibits several advantages compared to the use of sodium, such as higher solvability of lithium and higher melting point. As a result of the employment of lithium as tritium breeder and primary coolant in several designs of the deuterium fuelled thermonuclear reactor, the reactivity of lithium with other elements has been well investigated.[12–14] Accordingly, silicon, nitrogen, various metals as well as inorganic salts are soluble in liquid lithium at moderate temperatures,[13] which gives way to a promising approach to new nitridosilicates. Using this technique, we were able to synthesize a number of quaternary lithium nitridosilicates with varying degrees of condensation in lithium melts.[15–17] Group-like ($Li_4M_3Si_2N_6$ with M = Ca, Sr), chain-type ($LiCa_3Si_2N_5$, $Li_5Ln_5Si_4N_{12}$ with Ln = La, Ce) and framework nitridosilicates ($Li_2Sr_4Si_4N_8O$) can be obtained and hence the whole range of dimensionality can be accessed.[15,16,18] The reactions were conducted at temperatures below 1250 °C in liquid lithium in closed tantalum ampoules. However, we assume that upon varying the pressure conditions inside the ampoules by the amount of lithium azide/lithium nitride, the degree of condensation is influenced.

In this contribution we present a further new quaternary lithium nitridosilicate nitride obtained using liquid lithium

[a] Ludwig-Maximilians-Universität München, Department Chemie, Lehrstuhl für Anorganische Festkörperchemie, Butenandtstraße 5-13 (D), 81377 München, Germany
Fax: +49-89-2180-77440
E-mail: wolfgang.schnick@uni-muenchen.de

as fluxing agent. $Li_2Sr_4[Si_2N_5]N$ exhibits a two-dimensional $[Si_2N_5]^{7-}$ network and isolated N^{3-} ions, which have not been observed in nitridosilicates so far. However, they were found in nitridogallates, e.g. $Sr_6[GaN_3]N_2$ or nitridometallates, e.g. $Ca_6[MnN_3]N_2$.[19–21] Moreover, the nitridogermanate nitrides $M_7[GeN_4]N_2$ (M = Ca, Sr) have recently been structurally elucidated.[22]

Results and Discussion

Synthetical Approach

$Li_2Sr_4[Si_2N_5]N$ was obtained by the reaction of silicon diimide, lithium azide and strontium metal in liquid lithium in weld-shut tantalum ampoules at 900 °C. One equivalent cesium iodide is necessary for the reaction, probably acting as a catalyst for the formation of $Li_2Sr_4[Si_2N_5]N$. Cesium iodide might function as a template for the formation of the $[Si_2N_5]^{7-}$ network. The amount of CsI seems crucial as reactions with various other amounts do not lead to the slightly orange crystals of extremely air and moisture sensitive $Li_2Sr_4[Si_2N_5]N$.

Data Collection

Single-crystal X-ray structure analysis revealed a tetragonal body centered lattice. As Sr and Si atom positions can be described in a sub-cell, rather weak superstructure reflections in all three spatial directions had to be taken into account in the refinement, where the space group $I\bar{4}m2$ gave a reasonable structural model with satisfactory R values. Moreover, no evidence was found indicating a lower symmetry. In the tetragonal model, one nitrogen atom position is not included in the $[Si_2N_5]^{7-}$ silicate substructure, but corresponds to a discrete N^{3-} ion. The refinement of its site occupancy leads to an almost half-occupied site. In order to provide charge neutrality, the occupancy factor was fixed at a value of 1/2. There were no hints of a possible superstructure concerning the half-occupied nitrogen in the X-ray diffraction. Some details of the crystal structure determination are displayed in the experimental section. All atoms were refined anisotropically except the lithium and the half-occupied nitrogen atom position. Atomic coordinates and Wyckoff positions are listed in Table 1.

Table 1. Atomic coordinates and equivalent displacement parameters [Å^2] for $Li_2Sr_4[Si_2N_5]N$.

Atom		s.o.f	*x*	*y*	*z*	U_{eq}/U_{iso}[a]
Sr1	8*i*		0.24803(10)	0	0.08320(12)	0.0090(5)
Sr2	8*i*		0.24535(11)	1/2	0.09867(11)	0.0127(6)
Si	8*i*		0	0.2262(4)	0.2005(3)	0.087(7)
N1	8*i*		0	0.251(11)	0.0840(8)	0.014(3)
N2	4*e*		0	0	0.2305(11)	0.021(3)
N3	8*h*		0.1957(10)	0.3043(10)	1/4	0.025(2)
N4	8*i*	1/2	1/2	0.246(3)	0.090(2)	0.038(10)
Li	8*i*		1/2	0.2462(19)	0.2099(18)	0.011(5)

[a] U_{eq} is defined as 1/3 of the trace of the U_{ij} tensors; U_{eq} for N4 and Li.

Crystal Structure Description

The crystal structure of $Li_2Sr_4[Si_2N_5]N$ consists of loop-branched *dreier* single layers built up from $[Si_2N_5]^{7-}$ tetrahedra and can be derived from the apophyllite structure type $(KCa_4[Si_4O_{10}]_2(F,OH)\cdot 8H_2O)$,[24,25] although the molar ratio Si/N = 1:3 does not indicate a layered structure. This discrepancy is due to the discrete N^{3-} ions. The silicate substructure itself exhibits a condensation degree κ = 2:5, which is in accordance with a layered silicate structure. The layers in $Li_2Sr_4[Si_2N_5]N$ exhibit *vierer* and *achter* rings in analogy to the apophyllite structure[26] (cf. Figure 1) and are situated parallel (110). However, due to the higher symmetry of $Li_2Sr_4[Si_2N_5]N$ these rings are more regular and not tilted as in apophyllite. The distances Si–N range between 175.1(5)–176.7(13) pm and are in good accordance with other nitridosilicates.[27,28]

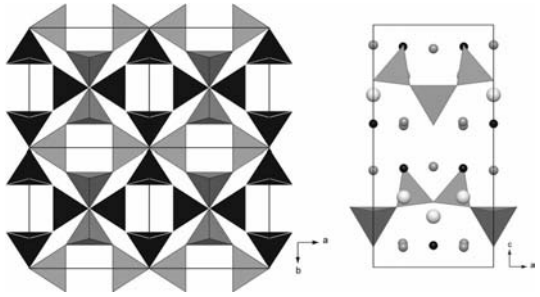

Figure 1. Left: $[SiN_4]$ substructure along [001], black $[SiN_4]$ tetrahedra in the back, gray ones in the front; right: unit cell along [010], Sr dark gray, Li white, N black.

There are two crystallographically independent Sr^{2+} positions occupying Wyckoff sites 8*i* (cf. Figure 2). The Sr1 positions exhibit a distorted octahedral coordination made up of nitrogen atoms. The Sr2 are surrounded by seven nitrogen atoms building a monocapped distorted octahedron. The distances within these coordination polyhedra range between 252.2(12) and 290.4(13) pm for Sr1 and 263.4(6)–274.3(3) pm for Sr2, respectively (cf. Table 2). These distances and coordination spheres correspond well with other strontium containing nitridosilicates (e.g. $SrSiN_2$, $SrYSi_4N_7$ or $Sr_2Si_5N_8$)[7,9,29] and the sum of the ionic radii according to Shannon[30] (264 pm sixfold coordination, 267 pm sevenfold coordination), Baur[31] (273 pm) and Slater[32]

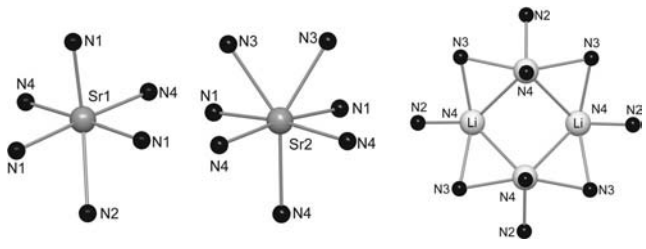

Figure 2. Coordination spheres of Sr1 (left), Sr2 (middle) and the Li atoms (right).

(265 pm). The Sr1 and Sr2 polyhedra are situated alternately in the crystal structure, forming double layers between the $[Si_2N_5]^{7-}$ layers.

Table 2. Selected interatomic distances [pm] for $Li_2Sr_4[Si_2N_5]N$. Standard deviations are given in parentheses.

Sr1–N1		252.2(12)	Sr2–N1	(2×)	263.4(6)
Sr1–N4	(2×)	265.4(18)	Sr2–N4	(2×)	270.0(18)
Sr1–N1	(2×)	265.4(6)	Sr2–N3		274.3(4)
Sr1–N2		290.4(13)	Sr1–N3		274.3(3)
Si–N3	(2×)	175.3(5)	Li–N4		181(4)
Si–N2		176.0(6)	Li–N2	(2×)	210.5(17)
Si–N4		176.8(13)	Li–N3		240.1(11)

The Li^+ site is coordinated by four nitrogen atoms with distances Li–N in the range 181(4)–240.1(11) pm (cf. Table 2). These distances are in good accordance with previously reported lithium nitridosilicates and the sum of the effective ionic radii (205–212 pm).[17,30–33] The coordination sphere of Li is unusual, because all ligands are rather on one side of the ion. However, there are several other examples for such a coordination, e.g. Li_2SiN_2 or $LiMo_2Ba_5N_7Cl_2$.[33,34] In the second coordination sphere, the lithium ions form $[Li_4N_8]^{20-}$ building units, which are separated by nitrogen from each other (cf. Figure 2). The distances Li–Li amounts to 288(3) pm, therefore no reasonable short pathways between the polyhedra indicative of lithium ion mobility, as, for example, described for Li_2SiN_2, can be found.[33]

The discrete N^{3-} ions (N4) are coordinated in a pseudo-octahedral way by five Sr^{2+} and one Li^+ (cf. Figure 3). The distances Sr–N^{3-} vary between 265.4(18) and 285(4) pm, which is within the range of comparable compounds[7,27] and correspond well with the sum of the ionic radii as described above.[30–32] The distance Li–N^{3-} of 181(4) pm is the shortest distance in the structure. Compared to the nitridogermanate nitride $Sr_7[GeN_4]N_2$, which exhibits discrete N^{3-} ions in addition to $[GeN_4]^{8-}$ tetrahedrons, the Sr–N^{3-} distances are in the same range.[22]

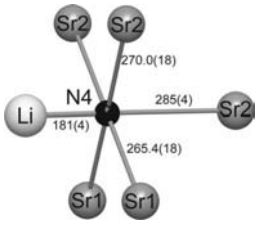

Figure 3. Coordination sphere of the half-occupied N^{3-} site with distances in pm.

Lattice Energy Calculations According to the MAPLE Concept

Lattice energy calculations (MAPLE: Madelung part of lattice energy)[30,35–37] were performed to prove the electrostatic consistency of the crystal structure and especially the presence of discrete N^{3-} ions. Hereby, exclusively electrostatic interactions in an ionic crystal were considered, depending on the charge, distance and coordination spheres of the constituting atoms. As there is no possibility to deal with partially occupied positions with the MAPLE program, it is necessary to use subgroup models for this calculation with fully occupied N^{3-} sites, although there are no indications for ordering from the X-ray diffraction data. Refinements in appropriate subgroups did not yield ordered models. Two subgroups of $I\bar{4}m2$ (no. 119) exhibit a splitting of the Wyckoff position 8*i*, which is occupied by N^{3-}, into two fourfold positions, namely $P\bar{4}m2$ (no. 115; k1) and *Imm*2 (44, t1). In both space groups, MAPLE calculations were performed with one N^{3-} site fully occupied and the other void. However, only in *Imm*2 reasonable partial MAPLE values could be achieved. Other arrangements of the voids in *Imm*2 and models in $P\bar{4}m2$ lead to negative partial MAPLE values and were therefore neglected. In order to have a higher diversity for the defect sites also calculations with enlarged unit cells were performed. In this context, space group *Imm*2 (**a**, 3**b**, **c**) also led to reasonable MAPLE values, with different arrangement of the voids. All MAPLE calculations in the space group *Imm*2 and *Imm*2 (**a**, 3**b**, **c**) gave reasonable MAPLE values, which were all in the same range, therefore only the results of the model in *Imm*2 are listed in Table 3. The calculated partialMAPLE values of the crystallographically independent atoms are in agreement with typical MAPLE ranges for different atom types of comparable compounds in the literature. Only the lithium position next to the defect sites is slightly below the expected range. The total MAPLE values correspond well with the sum of the total MAPLE values of the formally constituting compounds as can be seen in Table 3.

Table 3. Results of the MAPLE calculations [kJ/mol] for $Li_2Sr_4[Si_2N_5]N$ in space group *Imm*2 with half the isolated N^{3-} positions occupied, before and after optimization with VASP.[a]

	$Li_2Sr_4[Si_2N_5]N$	$Li_2Sr_4[Si_2N_5]N$ (after GGA optimization)
Sr^{2+}	1415, 1548, 2051, 2307	1587, 2121, 1764, 1969
Si^{4+}	9896, 9932	9899, 9824
$N^{[1]\,3-}$	4449, 4571	4476, 4655
$N^{[2]\,3-}$	4974, 5339, 5414	5431, 5368, 5259
$N^{[0]\,3-}$	3183	3455
Li^+	360, 679	539, 761
Total MAPLE	28245	28501
Δ	1.01%	0.10%

Total MAPLE ($1/2\ Li_4Sr_3Si_2N_6 + 1/2\ SrSiN_2 - 1/2\ Li_2SiN_2$): 28530 kJ/mol

[a] Typical partial MAPLE values [kJ/mol]: Sr^{2+}: 1500–2300, Si^{4+}: 9000–10200, $N^{[0]\,3-}$: 3000–3500, $N^{[1]\,3-}$: 4300–5000, $N^{[2]\,3-}$: 4600–6000, Li^+: 550–860.[22,37–39]

DFT Calculations

Structural optimizations of the four best models according to MAPLE calculations were calculated within the density functional theory (DFT) using the Vienna ab initio Simulation Package (VASP). The four models vary in the arrangement of the voids as depicted in Figure 4.

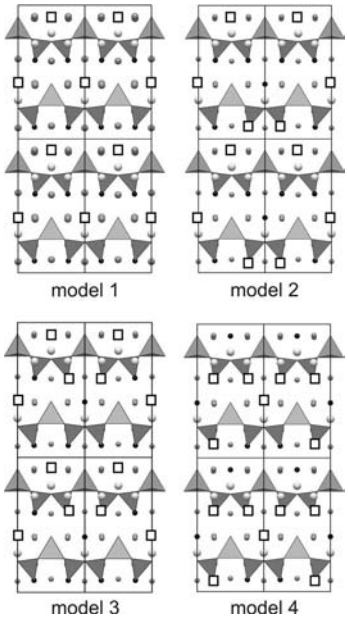

Figure 4. Depiction of the different models in the same unit cell for a better comparison. [model 1: *Imm*2; model 2–4: *Imm*2 (**a**, 3**b**, **c**)].

Structure optimizations of all four models show, that only minor deviations from the original cell and site parameters occurred during the optimizations. The optimized structures exhibit residual forces of less than 0.004 eV/Å. The cell volumes are in the same range for all models for the LDA as well as the GGA approximation. According to the lowest ground state energies, model 3, which exhibits the highest dispersion between the defect sites, is energetically favored (cf. Table 4). Also from a chemical point of view, this model is more likely, because an agglomeration of N^{3-} sites would lead to a high negatively charged location in the crystal structure, which is extremely unlikely to occur. However, the differences in energy are rather small and therefore indicate that all variants are likely to occur in the real structure.

Table 4. ΔE and V_0 of the optimized structural models compared to the MAPLE sums of the initial structures before optimization. The values of model 1 are adapted to the cells of the other models in *Imm*2_3*b* to have values better comparable.

	ΔE [eV][a]	V_0 [10^6 pm^3]	Δ MAPLE [%][b]
Model 1 (LDA)	1.511[c]	2517.15	1.01
Model 2 (LDA)	3.539	2538.67	2.56
Model 3 (LDA)	0	2521.90	1.34
Model 4 (LDA)	3.832	2540.59	2.57
Model 1 (GGA)	1.570[c]	2669.22	1.01
Model 2 (GGA)	3.145	2694.07	2.56
Model 3 (GGA)	0	2676.76	1.34
Model 4 (GGA)	3.477	2696.23	2.57

[a] Relative energies compared to the lowest energy of LDA method (–1107.935 eV) and GGA (–1003.197 eV). [b] Deviation from the theoretical MAPLE sums. [c] Convergence test was performed with a *Imm*2_3*b* cell for model 1 resulting ΔE = 1.505 (LDA) and ΔE = 1.564 (GGA).

DOS calculations for model 1, which exhibits the smallest unit cell, reveal a band gap of 0.37 eV. The band gap for model 3, which is energetically favored, is 0.38 eV. Although the models exhibit a different arrangement of the voids, the almost equal band gaps show, that it seems probable that in the real structure all models are present. The calculated band gaps are smaller than the expected ca. 2.2 eV corresponding to the slightly orange color and the transparency of the crystals. However, it is well known that band gaps are generally underestimated by DFT methods.[20,40]

Comparison between Lattice Energy Calculations and DFT Calculations

A comparison between the results of the DFT and the MAPLE calculations (cf. Table 4) leads to the conclusion that MAPLE can provide reasonable starting models, however, a prediction of the best model is not possible. MAPLE calculations of the optimized models revealed no significant differences. All LDA-optimized models had worse MAPLE values due to the fact that covalent bonding is overestimated by LDA and therefore slightly shorter, which has great influence on the MAPLE calculations. The GGA-optimized structures exhibit all less than 0.94% deviation from the theoretical MAPLE sums. In Table 3, the MAPLE values of the optimized model 1 are given in comparison to the values for the model derived by group-subgroup transformation. All partial values are in the expected range. Only the lithium position neighboring the void has a partial MAPLE value slightly below the expected range. However, respective values of other compounds, which exhibit low coordination for Li^+ range around 540 kJ/mol as well.[34,41]

Conclusions

In this contribution we present the first nitridosilicate nitride, namely $Li_2Sr_4[Si_2N_5]N$, with a layered $[Si_2N_5]^{7-}$ substructure, which can be derived from the apophyllite structure type. The title compound could be synthesized in closed tantalum ampoules using liquid lithium as fluxing agent. Apparently, the usage of cesium iodide as catalyst extends the spectrum of known quaternary lithium nitridosilicates. Therefore, we expect that a few more compounds can be afforded using lithium as fluxing agent and additional inorganic salts. To corroborate the half-occupied N^{3-} site MAPLE and DFT calculations were performed. In this context no higher ordering of the N^{3-} site could be found either in the X-ray diffraction or the DFT calculations. Moreover, $Li_2Sr_4[Si_2N_5]N$ is another example for the efficiency to develop new quaternary lithium nitridosilicates using liquid lithium. With respect to the highly anisotropic layered nitridosilicate structure and the concomitant presence of isolated N^{3-} ions, the high-pressure behavior of $Li_2Sr_4[Si_2N_5]N$ is of special interest as it might lead to a nucleophilic attack of the nitride ions at the Si tetrahedral centers.

Experimental Section

Synthesis: All manipulations were performed with rigorous exclusion of oxygen and moisture in flame-dried Schlenk-type glassware on a Schlenk line interfaced to a vacuum line (10^{-3} mbar) or in an argon-filled glove box (Unilab, MBraun, Garching, $O_2 < 0.1$ ppm, $H_2O < 0.1$ ppm). Argon (Messer–Griessheim, 5.0) was purified by passage through columns of silica gel (Merck), molecular sieves (Fluka, 4 Å), KOH (Merck, ≥ 85%), P_4O_{10} (Roth, ≥ 99%, granulate) and titanium sponge (Johnson Matthey, 99.5%, grain size ≤ 0.8 cm) at 700 °C. For the syntheses of the title compound tantalum tubes (wall thickness 0.5 mm, internal diameter 10 mm, length 300 mm) were cleaned and the oxide layer removed by treatment with a mixture of HNO_3 (concd.) and aqueous HF (40%). The tubes were weld-shut in an arc furnace under 1 bar of purified argon. During this procedure, the crucible holder was water cooled in order to avoid chemical reactions during welding.

For the synthesis of $Li_2Sr_4[Si_2N_5]N$, silicon diimide (38.7 mg, 0.67 mmol, synthesized according to literature[42]), LiN_3 (16.3 mg, 0.33 mmol, Sigma Aldrich 99.9%), Sr (59.9 mg, 0.68 mmol, Sigma Aldrich, 99.99%) and CsI (43.0 mg, 0.17 mmol, Sigma Aldrich, dried under vacuum) were mixed in an agate mortar, filled in a tantalum ampoule and covered with lithium (12 mg, 1.7 mmol, Alfa Aesar, 99.9%) in a glove box. The sealed tantalum ampoule was placed into a silica tube under argon, which was placed in the middle of a tube furnace. The temperature was raised to 900 °C (rate 5 °C min^{-1}), maintained for 24 h and cooled down to 500 °C (rate 0.2 °C min^{-1}). Subsequently, the sample was quenched to room temperature by switching off the furnace. The sample contained $Li_2Sr_4[Si_2N_5]N$ as orange highly air- and moisture-sensitive crytsals.

Chemical Analyses: Scanning electron microscopy was performed on a JEOL JSM-6500F equipped with a field emission gun at an acceleration voltage of 10 kV with a Si/Li EDX detector (Oxford Instruments, model 7418). Samples were prepared by placing single crystals on adhesive conductive pads and subsequently coating them with a thin conductive carbon film. Each EDX spectrum (Oxford Instruments) was recorded with the analyzed area limited onto one single crystal to avoid the influence of possible contaminating phases. EDX-analysis showed an atomic ratio Sr/Si = 1:1.7 which corroborates the formation of $Li_2Sr_4[Si_2N_5]N$.

Single Crystal X-ray Analysis: Single crystals of $Li_2Sr_4[Si_2N_5]N$ were isolated under a microscope, which is integrated in a glove box, enclosed in glass capillaries (Ø = 0.3 mm), and sealed under argon. Single-crystal X-ray diffraction data were collected at room temperature on a STOE IPDS I diffractometer (Stoe and Cie GmbH, Darmstadt) with Mo-K_α radiation (λ = 0.71073 Å, graphite monochromator). The structure was solved by direct methods after semi-empirical absorption correction. For the structure solution and refinement (see Table 5) the program package SHELX97 was used.[43]

Further details on the crystal structure investigation may be obtained from the Fachinformationszentrum Karlsruhe, 76344 Eggenstein-Leopoldshafen, Germany (Fax: +49-7247-808-666; E-mail: crysdata@fiz-karlsruhe.de), on quoting the depository number CSD-422596.

Computational Methods: Structural optimizations, total energies and band structure calculations are calculated within density functional theory (DFT)[44] using the Vienna ab initio Simulation Package (VASP). Hereby, the total energy pseudopotential method is combined with a plane-wave basis set.[45–48] The electron exchange and correlation energy were treated within the local-density approximation (LDA)[49] as well as generalized-gradient approximation (GGA)[50] together with the project-augmented wave (PAW) method.[51,52] The cut-off energy for the expansion of the wave function into the plane wave basis was 500 eV. For the Brillouin zone integration the Monkhorst–Pack scheme was used.[53] All residual forces were converged below 5×10^{-3} eV/Å^{-1}. For structural optimizations all internal and cell parameters as well as the unit cell volumes were relaxed for all used models. For the model with 56 atoms per unit cell (*Imm*2) a *k*-point mesh of $5 \times 5 \times 4$ was used for the models with 168 atoms per unit cell (*Imm*2_3*b*) $5 \times 3 \times 4$, respectively.

Table 5. Crystallographic data of $Li_2Sr_4[Si_2N_5]N$.

Formula	$Li_2Sr_4[Si_2N_5]N$
Formula mass [g mol^{-1}]	504.60
Crystal system	tetragonal
Space group	$I\bar{4}m2$ (no. 119)
Cell parameters [pm]	a = 751.46(11), c = 1508.9(3)
Cell volume [10^6 pm^3]	V = 852.0(2)
Formula units/cell	4
Crystal size [mm^3]	$0.09 \times 0.04 \times 0.01$
$\rho_{calcd.}$ [g cm^{-3}]	3.934
μ [mm^{-1}]	25.136
F(000)	912
Diffractometer	Stoe IPDS I
Temperature [K]	293(2)
Radiation, monochromator	Mo-K_α, (λ = 71.073 pm), graphite
Absorption correction	semi-empirical[23]
θ range [°]	2.7–27.5
Measured reflections	3500
Independent reflections	554
Observed reflections	499
Refined parameters	41
Flack parameter	0.50(4)
GoF	1.091
R indices [$F_o^2 \geq 2\sigma$ (F_o^2)]	R_1 = 0.0499, $wR2$ = 0.1364
R indices (all data)	R_1 = 0.0534, $wR2$ = 0.1413[a]
Max./min. residual electron density [e Å^{-3}]	3.72/–2.26

[a] $w = 1/[\sigma^2(F_o^2) + (0.0980\ P)^2 + 0.00\ P]^{-1}$, $P = (F_o^2 + 2\ F_c^2)/3$.

Acknowledgments

The authors are indebted Thomas Miller for recording the single X-ray data and Christian Minke for performing EDX measurements (all from the Department Chemie, University of Munich, LMU). Furthermore, we thank the Leibniz Rechenzentrum, Munich, for providing computer time on the Linux Cluster System. The authors gratefully acknowledge financial support from the Fonds der Chemischen Industrie (FCI) and the Deutsche Forschungsgemeinschaft (DFG), project SCHN 377/14–1.

[1] W. Schnick, *Angew. Chem.* **1993**, *105*, 846–858; *Angew. Chem. Int. Ed. Engl.* **1993**, *32*, 806–818.
[2] R.-J. Xie, N. Hirosaki, N. Kimura, K. Sakuma, M. Mitomo, *Appl. Phys. Lett.* **2006**, *90*, 191101/191101-191101/191103.
[3] M. Zeuner, S. Pagano, W. Schnick, *Angew. Chem.* **2011**, *123*, in press; *Angew. Chem. Int. Ed.* **2011**, *50*, in press.
[4] Superscripted numbers specify connectedness: number of directly connected silicon atoms.
[5] A. Weiss, A. Weiss, *Z. Anorg. Allg. Chem.* **1954**, *276*, 95–112.
[6] W. Schnick, H. Huppertz, *Chem. Eur. J.* **1997**, *3*, 679–683.
[7] T. Schlieper, W. Milius, W. Schnick, *Z. Anorg. Allg. Chem.* **1995**, *621*, 1380–1384.
[8] M. Woike, W. Jeitschko, *Inorg. Chem.* **1995**, *34*, 5105–5108.

[9] Z. A. Gál, P. M. Mallinson, H. J. Orchard, S. J. Clarke, *Inorg. Chem.* **2004**, *43*, 3998–4006.
[10] S. Esmaeilzadeh, U. Halenius, M. Valldor, *Chem. Mater.* **2006**, *18*, 2713–2718.
[11] H. Yamane, F. J. DiSalvo, *J. Alloys Compd.* **1996**, *240*, 33–36.
[12] R. J. Pulham, P. Hubberstey, *J. Nucl. Mater.* **1983**, *115*, 239–250.
[13] A. T. Dadd, P. Hubberstey, *J. Chem. Soc., Dalton Trans.* **1982**, 2175–2179.
[14] P. Hubberstey, P. G. Roberts, *J. Chem. Soc., Dalton Trans.* **1994**, 667–673.
[15] S. Pagano, S. Lupart, M. Zeuner, W. Schnick, *Angew. Chem.* **2009**, *121*, 6453–6456; *Angew. Chem. Int. Ed.* **2009**, *48*, 6335–6338.
[16] S. Lupart, M. Zeuner, S. Pagano, W. Schnick, *Eur. J. Inorg. Chem.* **2010**, 2636–2641.
[17] M. Zeuner, S. Pagano, S. Hug, P. Pust, S. Schmiechen, C. Scheu, W. Schnick, *Eur. J. Inorg. Chem.* **2010**, 4945–4951.
[18] S. Pagano, S. Lupart, S. Schmiechen, W. Schnick, *Z. Anorg. Allg. Chem.* **2010**, *636*, 1907–1909.
[19] G. Cordier, P. Höhn, R. Kniep, A. Rabenau, *Z. Anorg. Allg. Chem.* **1990**, *591*, 58–66.
[20] D. G. Park, Z. A. Gál, F. J. DiSalvo, *Inorg. Chem.* **2003**, *42*, 1779–1785.
[21] D. H. Gregory, M. G. Barker, P. P. Edwards, D. J. Siddons, *Inorg. Chem.* **1995**, *34*, 5195–5198.
[22] S. C. Junggeburth, O. Oeckler, D. Johrendt, W. Schnick, *Inorg. Chem.* **2008**, *47*, 12018–12023.
[23] *X.PREP*, Siemens Analytical X-ray Instruments Inc., Madison, Wisconsin, USA, **1996**.
[24] D. Mittra, S. Z. Ali, *J. Appl. Crystallogr.* **1976**, *9*, 54–56.
[25] F. Pechar, *Cryst. Res. Technol.* **1987**, *22*, 1041–1046.
[26] The terms *dreier* and *achter* rings were coined by Liebau and are derived from the German words "drei" (three) and "acht" (eight). However, for example a *dreier* ring is not a three-membered ring, but a six-membered ring comprising *three* tetrahedra centers.
[27] F. Stadler, O. Oeckler, J. Senker, H. A. Höppe, P. Kroll, W. Schnick, *Angew. Chem.* **2005**, *117*, 573–576; *Angew. Chem. Int. Ed.* **2005**, *44*, 567–570.
[28] W. Schnick, *Int. J. Inorg. Mater.* **2001**, *3*, 1267–1272.
[29] C. M. Fang, Y. Q. Li, H. T. Hintzen, G. d. With, *J. Mater. Chem.* **2003**, *13*, 1480–1483.
[30] R. D. Shannon, *Acta Crystallogr., Sect. A: Cryst. Found. Crystallogr.* **1976**, *32*, 751–767.
[31] W. H. Baur, *Crystallogr. Rev.* **1987**, *1*, 59–83.
[32] J. C. Slater, *J. Chem. Phys.* **1964**, *41*, 3199–3204.
[33] S. Pagano, M. Zeuner, S. Hug, *Eur. J. Inorg. Chem.* **2009**, 1579–1584.
[34] A. Gudat, R. Kniep, J. Maier, *Z. Naturforsch., Teil B* **1992**, *47*, 1363–1366.
[35] R. Hübenthal, Vers. 4 ed., University of Gießen, **1993**.
[36] R. Hoppe, *Angew. Chem.* **1966**, *78*, 52–63; *Angew. Chem. Int. Ed. Engl.* **1966**, *5*, 95–106.
[37] R. Hoppe, *Angew. Chem.* **1970**, *82*, 7–16; *Angew. Chem. Int. Ed. Engl.* **1970**, *9*, 1925–1934.
[38] H. A. Höppe, Doctoral Thesis, University of Munich, **2003**.
[39] K. Köllisch, Doctoral Thesis, University of Munich, **2001**.
[40] C. Braun, M. Seibald, S. L. Börger, O. Oeckler, T. D. Boyko, A. Moewes, G. Miehe, A. Tücks, W. Schnick, *Chem. Eur. J.* **2010**, *16*, 9646–9657.
[41] R. Marx, R. M. Ibberson, *J. Alloys Compd.* **1997**, *261*, 123–131.
[42] H. Lange, G. Wötting, G. Winter, *Angew. Chem.* **1991**, *103*, 1606–1625; *Angew. Chem. Int. Ed. Engl.* **1991**, *30*, 1579–1597.
[43] G. M. Sheldrick, *Acta Crystallogr., Sect. A* **2008**, *64*, 112–122.
[44] P. Hohenberg, W. Kohn, *Phys. Rev. B* **1964**, *136*, 864–871.
[45] G. Kresse, J. Hafner, *Phys. Rev. B* **1996**, *47*, 558–561.
[46] G. Kresse, J. Hafner, *Phys. Rev. B* **1994**, *49*, 14251–15269.
[47] G. Kresse, J. Furthmüller, *Comput. Mater. Sci.* **1996**, *6*, 15–50.
[48] G. Kresse, J. Furthmüller, *Phys. Rev. B* **1996**, *54*, 11169–11186.
[49] J. P. Perdew, A. Zunger, *Phys. Rev. B* **1981**, *23*, 5048–5079.
[50] J. P. Perdew, J. A. Chevary, S. H. Vosko, K. A. Jackson, M. R. Pederson, D. J. Singh, C. Fiolhais, *Phys. Rev. B* **1992**, *46*, 6671–6687.
[51] P. E. Blöchl, *Phys. Rev. B* **1994**, *50*, 17953–17979.
[52] G. Kresse, J. Joubert, *Phys. Rev. B* **1999**, *59*, 1758–1775.
[53] H. J. Monkhorst, J. D. Pack, *Phys. Rev. B* **1976**, *13*, 5188–5192.

Received: February 3, 2011
Published Online: March 16, 2011

